Simulation of Swimming Organisms: Coupling Internal Mechanics with External Fluid Dynamics

Ricardo Cortez
Department of Mathematics
Tulane University
New Orleans, LA 70118
and
Nathaniel Cowen
Courant Institute of Mathematical Sciences
251 Mercer Street
New York, NY 10012
and
Robert Dillon
Department of Pure and Applied Mathematics
Washington State Universiy
Pullman, WA 99164
and
Lisa Fauci
Deparment of Mathematics
Tulane University
New Orleans, LA 70118

December 4, 2003

1 Abstract

Problems in biological fluid dynamics typically involve the interaction of an elastic structure with the surrounding fluid. Motile spermatozoa in the reproductive tract and swimming leeches are examples of such fluid-structure interactions. We describe a unified computational approach, based upon an immersed boundary framework, that couples internal force generating mechanisms of organisms and cells with an external, viscous, incompressible fluid. Many aspects of internal force generation mechanisms are not completely understood. It is our goal to use computational simulations to examine biological hypotheses regarding these mechanisms. We present recent progress on coupling internal molecular motor mechanisms of beating cilia and flagella with an external fluid, as well as coupling muscle mechanics with fluid dynamics in three dimensional undulatory swimming of nematodes and leeches.

2 Introduction

Computational simulations, in conjunction with laboratory experiments, can provide valuable insight into complex biological systems that involve the interaction of an elastic structure with a viscous, incompressible fluid. The setting of biological fluid dynamics presents a number of challenges in addition to those traditionally faced in computational fluid dynamics. Dynamic flow situations dominate and it is necessary to capture time-dependent geometries with large structural deformations. In addition, the shape of the elastic structures are not preset, but determined by the fluid dynamics.

The Reynolds number of a flow is a dimensionless parameter that measures the relative significance of inertial forces to viscous forces. Due to the small length scales, the swimming of microorganisms corresponds to very small Reynolds numbers ($10^{-6} - 10^{-2}$). Faster and larger organisms like fish and eels swim at high Reynolds number ($10^2 - 10^5$). However, other swimming organisms like nematodes and tadpoles experience inertial forces comparable to viscous forces, and swim at Reynolds numbers of order one.

We use modern methods in computational fluid dynamics to create a controlled environment where the measurement and visualization of the fluid dynamics of swimming organisms can be made. We have designed a unified computational approach, based upon an immersed boundary framework [1], that couples internal force generation mechanisms of organisms and cells with an external, viscous, incompressible fluid. This approach can be applied to model low, moderate, and high Reynolds number flow regimes.

Analyzing the fluid dynamics of a flexible, swimming organism is very difficult, even when an organism's waveform is assumed to be known in advance [2, 3]. In the case of microorganism motility, the low Reynolds number does simplify the mathematical analysis since the equations of fluid mechanics in this regime are linear. However, even at low Reynolds numbers, the waveform of a microorganism is an emergent property of the coupled nonlinear system consisting of the organism's force generation mechanisms, its passive elastic structure, and the external fluid dynamics.

In the immersed boundary framework, the force generating organism is accounted for by suitable contributions to a force term in the fluid dynamic equations. The force of an organism on the fluid is a Dirac delta-function layer of force supported only by the region of

fluid which coincides with material points of the organism; away from these points this force is zero. After including this force distribution on the fluid, we solve the fluid equations using either a finite difference grid-based method or the *Regularized Stokeslets* grid-free method developed specifically for zero Reynolds number regimes [4].

Below we present recent progress on coupling internal molecular motor mechanisms of beating cilia and flagella with an external fluid, as well as three dimensional undulatory swimming of nematodes and leeches. We expect these computational models to provide a testbed where different theories of internal force generation mechanisms may be examined.

3 Immersed boundary framework

The immersed boundary method was introduced by Charles Peskin [1] to model blood flow in the heart. This method has been advanced to study other biofluiddynamic problems including platelet aggregation, three-dimensional blood flow in the heart, dynamics of the inner ear, blood flow in the kidney, limb development and deformation of red blood cells. For a recent overview, see [1].

We will describe the immersed boundary method in the context of swimming organisms. We regard the fluid as viscous and incompressible, and the filaments that comprise the organisms as elastic boundaries immersed in this fluid. In our three-dimensional simulations, many filaments join together to form the organism. A typical three-dimensional structure is shown in Figure 1. This nematode, tapered at both ends, is built out of three families of filaments: circular, longitudinal, and right- and left-handed helical filaments.

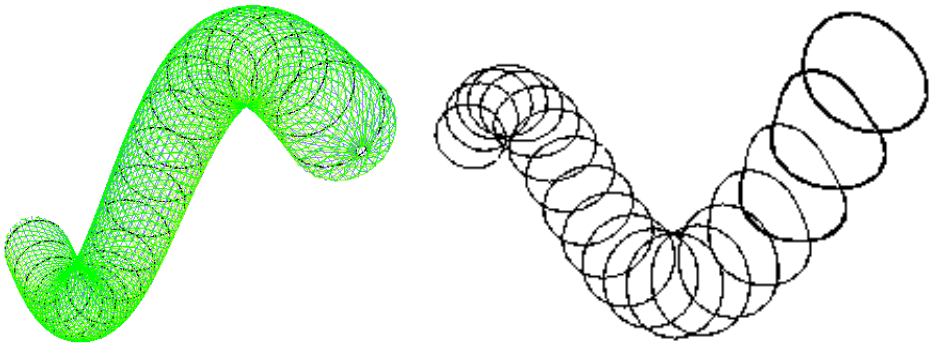

Figure 1: (a) An immersed boundary nematode. (b) A snapshot of a swimming nematode suppressing all but the 'circular' fibers. Notice that these fibers are elastic and deform in response to the viscous fluid.

We assume that the flow is governed by the incompressible Navier-Stokes equations (conservation of momentum and conservation of mass):

$$\rho\left[\frac{\partial \mathbf{u}}{\partial t} + \mathbf{u}\cdot\nabla\mathbf{u}\right] \;=\; -\nabla p + \mu\Delta\mathbf{u} + \mathbf{F}(\mathbf{x},t)$$

$$\mathbf{F} = \sum_k \mathbf{F^k}$$

$$\nabla \cdot \mathbf{u} = 0.$$

Here ρ is the fluid density and μ is the dynamic viscosity, $\mathbf{u}$ is the fluid velocity, p denotes the pressure, and $\mathbf{F}$ is the force per unit volume which is exerted on the fluid by the organism. This force is split into the contributions from each of the filaments comprising the organism. The forces $\mathbf{F^k}$ due to the kth filament include the elastic forces due to the individual filament structures, the passive elastic forces due to links between filaments, and may include active forces due to muscle contractions (in the case of nematode or leech swimming) or active forces due to the action of dynein molecular motors (in the case of ciliary and flagellar beating). $\mathbf{F}$ is a δ-function layer of force supported only by the region of fluid which coincides with material points of the filaments; away from these points the force is zero.

Let $\mathbf{X}^k(s,t)$ denote the kth filament as a function of a Lagrangian parameter s and time t and let $\mathbf{f}^k(s,t)$ denote the boundary force per unit length along the kth filament. The boundary force depends upon the biological system being modelled, but the general form will be discussed below. The elastic boundary is assumed to have the same density as the surrounding fluid, and its mass is attributed to the mass of the fluid in which it sits, and thus the forces are transmitted directly to the fluid. The force field $\mathbf{F^k}$ from the filament $\mathbf{X}^k(s,t)$ is therefore:

$$\mathbf{F^k}(\mathbf{x},t) = \int \mathbf{f^k}(s,t)\delta(\mathbf{x} - \mathbf{X^k}(s,t))ds.$$

Here the integration is over the kth one-dimensional filament comprising an immersed boundary, and δ is the three-dimensional Dirac delta-function. The total force $\mathbf{F}(\mathbf{x},t)$ is calculated by adding the forces from each of the filaments.

Each filament of the immersed boundary is approximated by a discrete collection of points. This boundary exerts elastic forces on the fluid near each of these points. We imagine that between each pair of successive points on a filament, there is an elastic spring or 'link' which generates forces to push the link's length toward a specified resting length. The force arising from the spring on a short filament segment of length ds is the product of a stiffness constant and the deviation from rest length. This force is approximated by the force density at a single point in the segment times ds. In addition to the forces due to springs along individual filaments, forces due to passive or active interactions between filaments contribute to the force density. Each spring may have a time-dependent rest length, as well as a time-dependent stiffness. Our coupled fluid-immersed boundary system is closed by requiring that the velocity of a material point of a filament be equal to the fluid velocity evaluated at that point.

Grid-based immersed boundary algorithm

We can summarize the immersed boundary algorithm as follows: Suppose that at the end of timestep n we have the fluid velocity field $\mathbf{u}^n$ on a grid, and the configuration of the immersed boundary points on the filaments comprising the organism $(\mathbf{X^k})^n$. Then to advance the system by one timestep we must:

1. Calculate the force densities $\mathbf{f^k}$ from the boundary configuration;
2. Spread the force densities to the grid to determine the forces $\mathbf{F^k}$ on the fluid;
3. Solve the Navier-Stokes equations for $\mathbf{u}^{n+1}$;
4. Interpolate the fluid velocity field to each immersed boundary point $(\mathbf{X^k})^n$ and move the point at this local fluid velocity.

The crucial feature of this algorithm is that the immersed boundary is *not* the computational boundary in the Navier-Stokes solver. It is a dynamic force field which influences the fluid motion through the force term in the fluid equations. The Navier-Stokes equations are solved on a regular grid with simple boundary conditions in Step 3. In addition, this modular approach allows us to choose a fluid solver best suited to the Reynolds number of the problem. This solver can be based upon a variety of formulations, including finite difference and finite element methods. Steps (2) and (4) involve the use of a discrete delta function which communicates information between the grid and the immersed boundary points [1].

Grid-free method of Regularized Stokeslets

At the low Reynolds number regime of microorganism swimming, we may alternatively describe the fluid dynamics using the quasi-steady Stokes equations:

$$\begin{aligned} \mu\Delta\mathbf{u} &= \nabla p - \mathbf{F}(\mathbf{x},t) \\ \nabla\cdot\mathbf{u} &= 0. \end{aligned}$$

A fundamental solution of these equations is called a Stokeslet, and it represents the velocity due to a concentrated force acting on the fluid at a single point in an infinite domain of fluid [3]. In fact, $\mathbf{F}(\mathbf{x},t)$ is the sum of such point forces. In [4], Ricardo Cortez considered the smoothed case where the concentrated force is applied not at a single point, but over a small ball of radius ϵ centered at the immersed boundary point. A regularized fundamental solution or *regularized Stokeslet* may be computed analytically. The method of regularized Stokeslets is a Lagrangian method in which the trajectories of fluid particles are tracked throughout the simulation. The method is particularly useful when the forces that drive the fluid motion are placed along the surface of a swimming organism that deforms due to its interaction with the fluid. The forces on the surface are given by regularized delta functions and the resulting velocity represents the exact solution of Stokes equations for the given forces.

Since the incompressible Stokes equations are linear, one may use direct summation to compute the velocity at each of the immersed boundary points in order to advance a time step. This method of regularized Stokeslets is related to boundary integral methods, but has the advantage that forces may be applied at any discrete collection of points. These points need not approximate a smooth interface.

We have successfully implemented this algorithm for ciliary beating in two dimensions, and helical swimming in three dimensions. Figure 2 shows a snapshot of a helical swimmer with fluid velocity fields computed along two planes perpendicular to the axis of the helix.

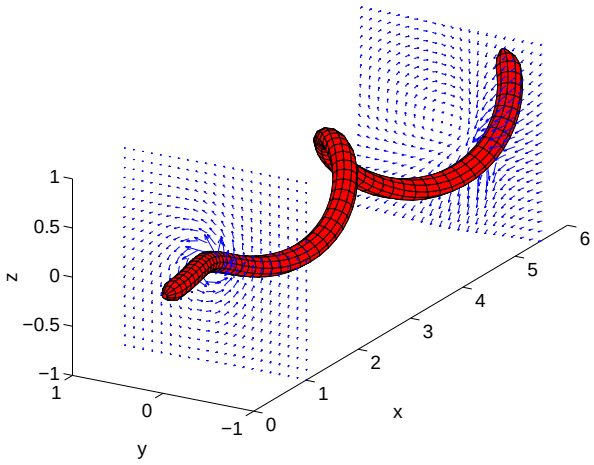

Figure 2: A snapshot of a bacterium swimming due to propagation of a helical wave. Fluid velocity vectors are shown on two planes perpendicular to the swimming axis. The simulation used the grid-free method of Regularized Stokeslets.

4 Undulatory swimming

Nematodes are unsegmented roundworms with elongated bodies, tapered at both ends. The most famous nematode is *C. Elegans*, a model organism for genetic, developmental and neurobiological studies. Nematodes possess a fluid-filled cavity, longitudinal muscles and a flexible outer cuticle that is composed of left- and right-handed helical fibers, and maintain a circular cross-section. The alternate contractions of their dorsal and ventral longitudinal muscles cause these worms to swim with an eel-like, undulatory pattern [5]. A typical nematode is about $.5 - 1$ milimeter long, and undulates with a wavespeed between $.8 - 4$ milimeters per second. Therefore, in water, nematode swimming is governed by a Reynolds number (based upon wavelength and wavespeed) between $.4 - 4$.

The filaments comprising our computational organism were chosen to reflect the anatomy of the nematode, including the longitudinal muscle fibers and the helical fibers of its cuticle. The stiffness constants of the 'springs' making up these fibers may be chosen to reflect the elastic properties of the tissue. In the simulation depicted in Figure 1, sinusoidal undulatory waves are passed along the body of the immersed organism by imposing appropriate muscle contractions along its longitudinal and helical filaments. Figure 3 shows a three-dimensional perspective of the worm along with the velocity field of the fluid depicted in the plane determined by its centerline. (Here a grid-based immersed boundary algorithm was used.) The flow field shows vortices of alternating direction that are supported along the length of the organism. This characteristic flow pattern was experimentally observed for the nematode *Turbatrix* in [5]. The swimming speed of this simulated nematode, whose amplitude of oscillation was chosen to be about one half of that reported for *Turbatrix*, was computed to be five percent of the propulsive wave speed along its body. These calculations compare very well with the experimentaly observed swimming speed of twenty percent of wave speed reported for *Turbatrix* [5], since swimming speed is proportional to the square of the amplitude of the

wave [2].

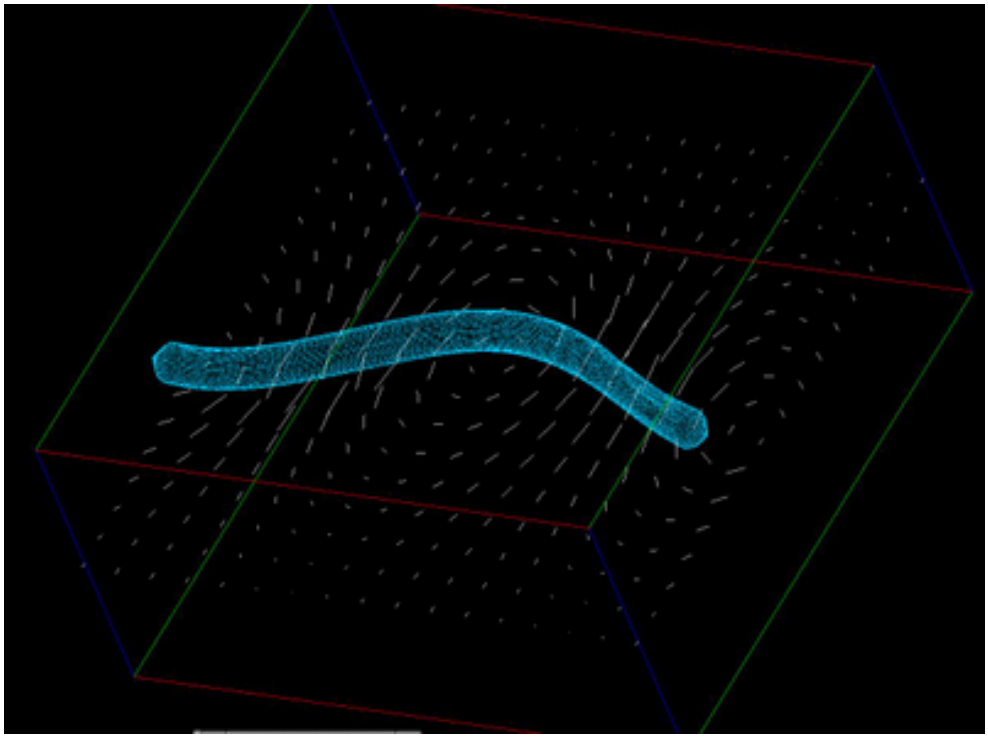

Figure 3: Snapshot of a swimming nematode shown with velocity field.

We now turn to modeling another undulatory swimmer - the leech. Leeches are larger and faster than nematodes, and have an elliptical rather than a circular cross-section. We focus on 2 centimeter long juvenile leeches, with propulsive wave speeds of approximately 5 centimeters per second undulating in water. In this case, the Reynolds number based upon wavelength and wavespeed is about 1000 - inertial effects are significantly more important than viscous effects [6].

Using the same immersed boundary construct as we did for the nematodes (longitudinal muscle fibers, right- and left-helical fibers), but replacing the circular fibers with elliptical cross-sectional fibers, we examine the leech's undulatory swimming in a 3D fluid. Figure 4 shows four snapshots of the leech as viewed from the side, along with fluid markers for flow visualization. Each of the four snapshots depicts the leech at the same phase in its undulation, during successive periods. A wave passed over the body from left to right. Note the forward swimming progression, and the wake that is left behind. The red fluid markers in the foreground were initially placed far enough from the side of the leech that they are not carried with the organism. Figure 5 shows four snapshots of the leech from a different perspective. Note the complex three- dimensional particle mixing that occurs.

For our simulated leech, we have used the experimental data on waveform and wavespeed reported by Jordan on the juvenile leech in [6]. Because of accuracy constraints that require enough grid points within a cross-section of the leech, the aspect ratio of the elliptical cross-section of the simulated leech is $2:1$, and not the actual $5:1$ as reported in [6]. We believe

that this difference is causing the simulated leech to swim about five times slower than the real leech.

5 Cilia and flagella

Cilia and flagella are the prominent organelles associated with the motility of microorganisms. Although the patterns of flagellar movement are distinct from those of ciliary movement, and the flagella are typically much longer than cilia, their basic ultrastructure is identical. The bending of cilia and flagella is produced by a core which is called the axoneme. The typical 9+2 axoneme consists of a central pair of single microtubules surrounded by nine outer doublet microtubules and encased by the cell membrane (cf [7, 8] for review). Radial spokes attach to the peripheral doublet microtubules and span the space toward the central pair of microtubules. The outer doublets are connected by nexin links between adjacent pairs of doublets. Two rows of dynein arms extend from the A-tubule of an outer doublet toward the B-tubule of an adjacent doublet at regularly spaced intervals. The bending of the axoneme is caused by sliding between pairs of outer doublets, due to the unidirectional ATP-induced force generation of the dynein molecular motors. *The precise nature of the spatial and temporal control mechanisms regulating the various waveforms of cilia and flagella is still unknown.*

Considerable interest has been focused on the development of mathematical models for the hydrodynamics of individual as well as rows of cilia and on individual flagellated organisms. The resistive-force theory of Gray and Hancock [9] and the slender body theory of Lighthill [3] are particularly noteworthy. More detailed hydrodynamic analysis, such as refined slender body theory and boundary element methods, have produced excellent simulations of both two- and three-dimensional flagellar propulsion and ciliary beating in an infinite fluid domain or in a domain with a fixed wall. In all of these fluid dynamical models, the shape of the ciliary or flagellar beat was taken as given. More recent work by Gueron and Levit-Gurevich have included a model that addresses the internal force generation in a cilium [10], but do not explicitly model the individual microtubule-dynein interactions.

We have developed a model for an individual cilium or flagellum that incorporates discrete representations of the dynein arms, the passive elastic structures of the axoneme including the microtubules and nexin links, as well as the surrounding fluid. This model couples the internal force generation of the molecular motors through the passive elastic structure with the external fluid mechanics. Detailed geometric information is available, such as the spacing and shear between the microtubules, the local curvature of individual microtubules and the stretching of the nexin links. In addition, the explicit representation of the dynein motors allows us the flexibility to incorporate a variety of activation theories. **The ciliary beat or flagellar waveform is not preset, but is an emergent property of the interacting components of the coupled fluid-axoneme system.**

In [11, 12] we presented a model of a simplified axoneme consisting of two microtubules. Dynein motors are represented as dynamic, diagonal elastic links between the two microtubules. In order to achieve beating in the simplified two-microtubule model, we allow two

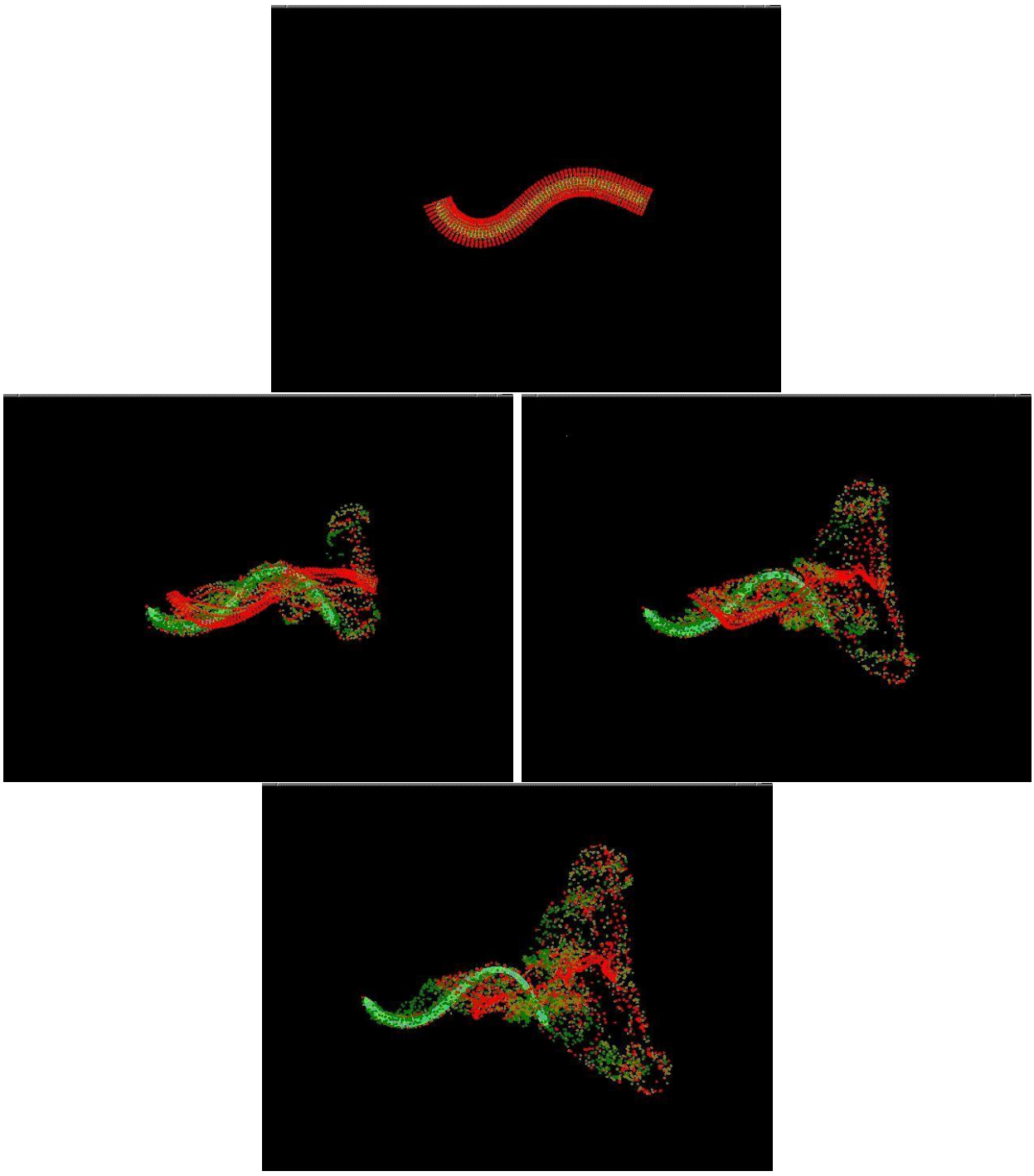

Figure 4: Snapshots of leech and surrounding fluid markers at the same phase in its undulation during successive temporal periods. The actual organism is mostly obscured in the first panel by the fluid markers placed around it.

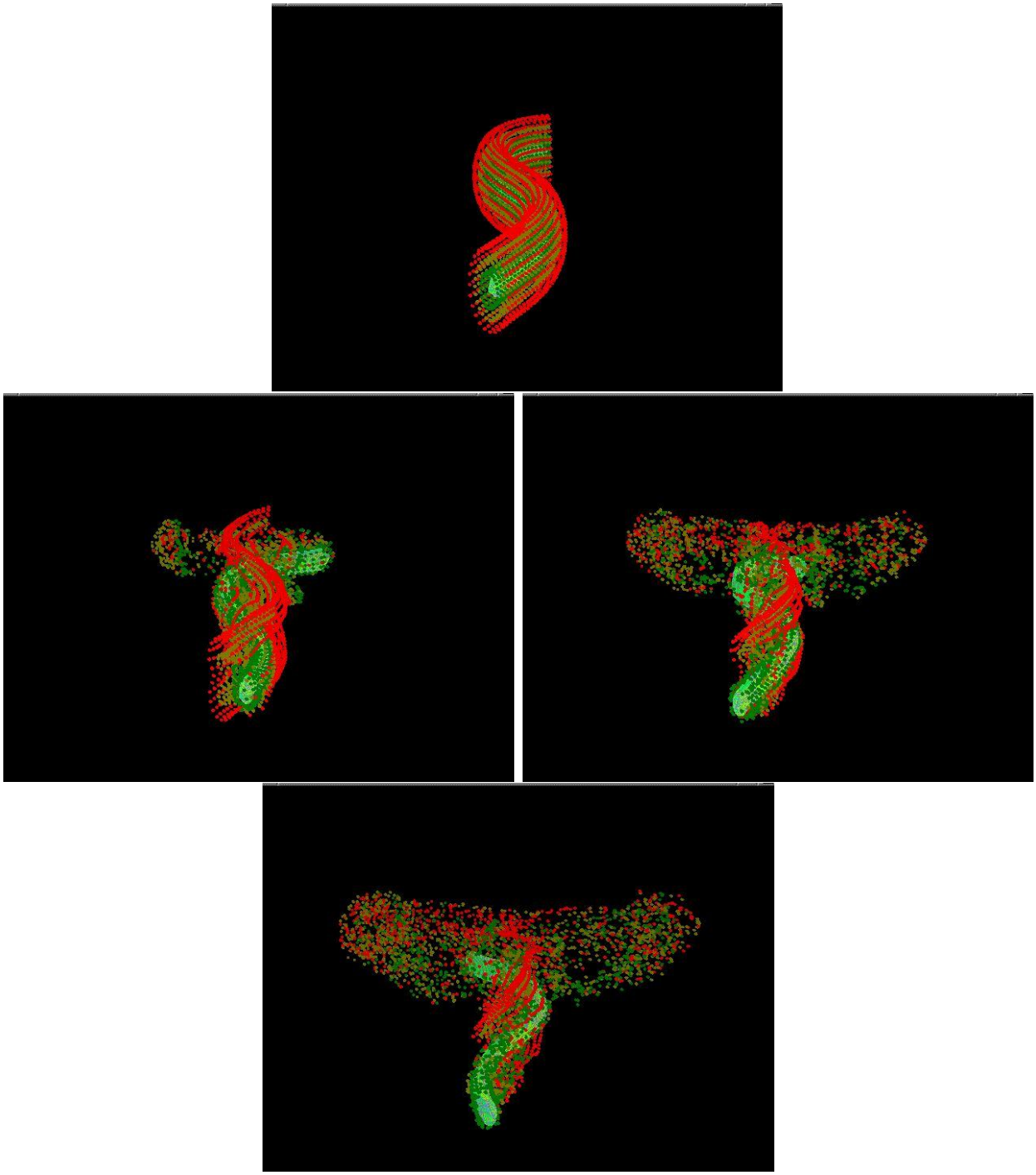

Figure 5: Snapshots of leech and surrounding fluid markers. From this perspective, the wave is moving back over the body, and the swimming progression is towards the viewer. Note the complex three-dimensional fluid mixing depicted by the evolution of the fluid markers.

sets of dyneins to act between the microtubules - one set is permanently attached to fixed nodes on the left microtubule, and the other set to fixed nodes on the right. Contraction of the dynein generates sliding between the two microtubules. In either configuration, one end of a dynein can attach, detach, and reattach to attachment sites on the microtubule. Dynein connectivity is reassessed at each time step of a numerical simulation. As the microtubules slide, the endpoint of a dynein link may 'ratchet' from one node of the microtubule to another.

Each microtubule is modeled as a pair of filaments with diagonal cross-links. Resistance to bending of the microtubules is governed by the elastic properties of the diagonal cross-links. Adjacent pairs of microtubules are interconnected by linear elastic springs representing the nexin and/or radial links of the axoneme. In the case of ciliary beating, the axoneme is tethered to fixed points in space via strong elastic springs at the base. The entire structure is embedded in a viscous incompressible fluid.

Figure 6 shows a cilium during the power stroke (note the two microtubules) and a ciliary waveform showing a single filament at equally spaced time intervals. This waveform was not preset, but resulted from the actions of individual dynein motors. In particular, the activation cycle of each dynein motor along the cilium was determined by the local curvature of the cilium. Figure 7 shows the swimming of a model sperm cell whose waveform is also the result of a curvature control model. The beating cilium does, indeed, result in a net displacement of fluid in the direction of the power stroke, and the sperm cell does indeed, swim in the direction opposite that of the wave. We have shown in [12] that making different assumptions about the internal dynein activation mechanisms does, indeed, result in different swimming behavior. In particular, when the curvature control model is altered to change the effective time scale of dynein kinetics, the time of a single beat changes significantly, along with the entire waveform of the flagellum.

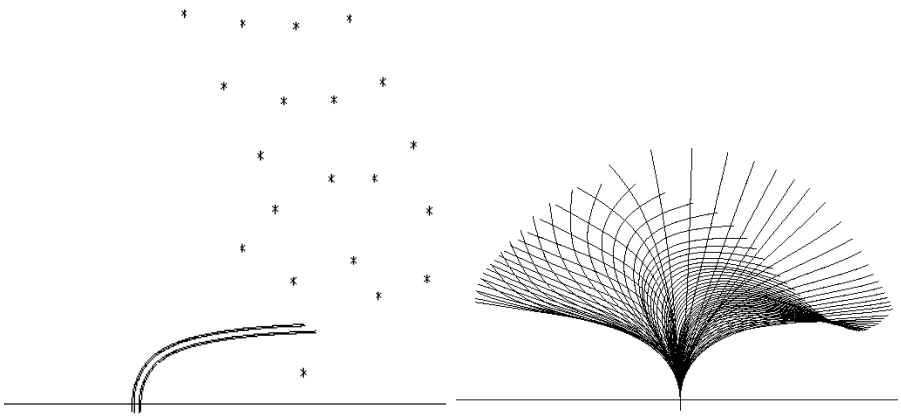

Figure 6: (a) A two-microtubule cilium nearing the end of its power stroke. Fluid markers are denoted by asterisks. These were placed initially directly above the base of the cilium in a rectangular array. The displacement to the right is the result of the net fluid flow induced by the beating cilium. (b) A ciliary waveform showing a single filament at equally spaced time intervals.

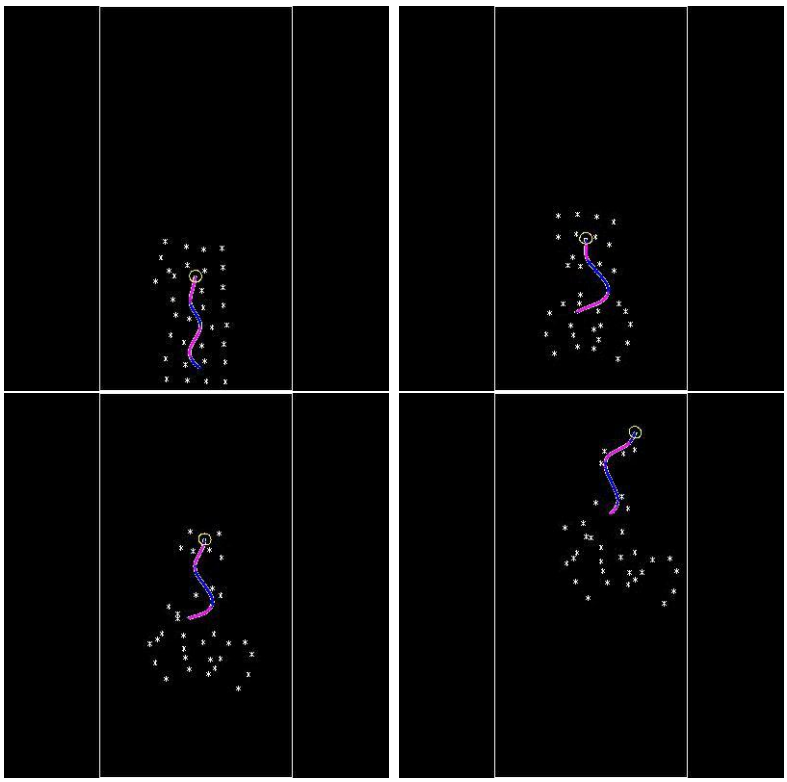

Figure 7: A sequence of a two-microtubule sperm cell swimming upwards as a wave passes from base to tip. The red (blue) color indicates that the right (left) family of dyneins are activated at that position of the flagellum. Fluid markers are denoted by asterisks.

6 Conclusions

Computational fluid dynamics along with biological modeling provides a powerful means for studying the internal force generation mechanisms of a swimming organism that are necessarily coupled with the surrounding fluid. The integrative approach presented here allows us to use computer simulations to examine theories of physiological processes such as dynein activation in a beating cilium, and muscle dynamics in invertebrates. The success of these models depends both upon the continued development of robust and accurate numerical methods, and the interdisciplinary collaboration of computational scientists and biologists.

References

[1] Peskin, C.S., 2002. The immersed boundary method. Acta Numerica, 11:479-517.

[2] Childress, S., 1981. Mechanics of Swimming and Flying. Cambridge University Press.

[3] Lighthill, J.L., 1975. Mathematical Biofluiddynamics. SIAM Vol. 17, Regional Conference Series in Applied Mathematics.

[4] Cortez, R., 2001. The method of regularized Stokeslets. SIAM J. Sci. Comput., 23, no. 4: 1204-1225.

[5] Gray, J. and H. W. Lissmann, 1964. The locomotion of nematodes. J. Exp. Biol., 41: 135-154.

[6] Jordan, C.E., 1998. Scale effects in the kinematics and dynamics of swimming leeches. Can. J. Zoology, 76:1869-1877.

[7] Murase, M. The Dynamics of Cellular Motility. John Wiley , Chichester, 1992.

[8] Witman, G.B. Introduction to Cilia and Flagella, in Ciliary and Flagellar Membranes (R. A. Bloodgood, ed.), Plenum, New York, (1990), p. 1-30.

[9] Gray, J. and G. Hancock, 1955. The propulsion of sea-urchin spermatozoa. J. Exp. Biol., 32: p. 802-814.

[10] Gueron, S. and K. Levit-Gurevich, 1998. Computation of the internal forces in cilia: Application to ciliary motion, the effects of viscosity, and cilia interactions. Biophys. J., 74: p. 1658-1676.

[11] Dillon, R. and L.J. Fauci, 2000. An integrative model of internal axoneme mechanics and external fluid dynamics in ciliary beating. J. Theor. Biol., 207: p. 415 - 430.

[12] Dillon, R., Fauci, L.J., and C. Omoto, 2002. Mathematical modeling of axoneme mechanics and fluid dynamics in ciliary and sperm motility. Dynamics of Continuous, Discrete and Impulsive Systems, to appear.